Interaction Notes

Note 196

September 1974

THE CROSSED-DIPOLE STRUCTURE OF AIRCRAFT IN AN ELECTROMAGNETIC PULSE ENVIRONMENT

Robert W. Burton

Naval Postgraduate School
Monterey, California

ABSTRACT

The crossed-dipole receiving antenna has been used as a representative model to approximate electromagnetic pulse effects on aircraft. This paper presents significant experimental and theoretical advances which correctly describe the electromagnetic properties of the crossed-dipole receiving antenna illuminated by a monochromatic source. Results are presented for electrically moderately thin structures.

In practice, when a crossed-dipole receiving antenna is excited by a broad spectrum electromagnetic pulse, certain important electrical resonances occur: that is, at specific single frequencies of excitation some portions of the structure can support large amplitude standing aves of current and/or charge. Under such conditions a current maximum/charge minimum, current minimum/charge minimum, or current minimum/charge maximum may occur at the junction region. Examples of resonant and antriresonant situations for the parasitic monopole and the crossed dipole which highlight the possible interactions between the arms of the crossed dipole are presented which give insight into methods of analyzing aircraft in an electromagnetic pulse environment.

TABLE OF CONTENTS

I. Introduction

For some time there has been considerable interest (Taylor, C. D., 1969; Taylor, C. D. et al., 1970; Butler, C. M., 1972; Chao, H. H. and Strait, B. J., 1972) in utilizing the high-speed digital computer in the theoretical study of electromagnetic scattering from arbitrary configurations of relatively thin cylindrical wires both from the point of view of determining the radar cross section of the scatterers as well as their coupling to the electromagnetic field through induced charges and currents. Inevitably, this process leads to assumptions of boundary conditions in the vicinity of the junction and the realization that thin wire theory (Mei, K. K., 1965) does not apply in this region. The essence of this nonapplicability lies in the fact that there is not rotational symmetry in the region closer than $\lambda/10$ from the junction with the result that measured charge and current densities presented in this paper differ significantly from results predicted using thin wire theory both in the junction region as well as along the entire structure.

In order to gain insight into junction effects, experiments were performed to measure the induced surface charge and current distributions on both the simple receiving monopole mounted over a conducting ground plane and the crossed-dipole receiving antenna likewise mounted over a conducting ground plane (figure 1). In each case the receiving structure was illuminated by a vertically polarized, monochromatic incident plane wave. Using various arm lengths on the

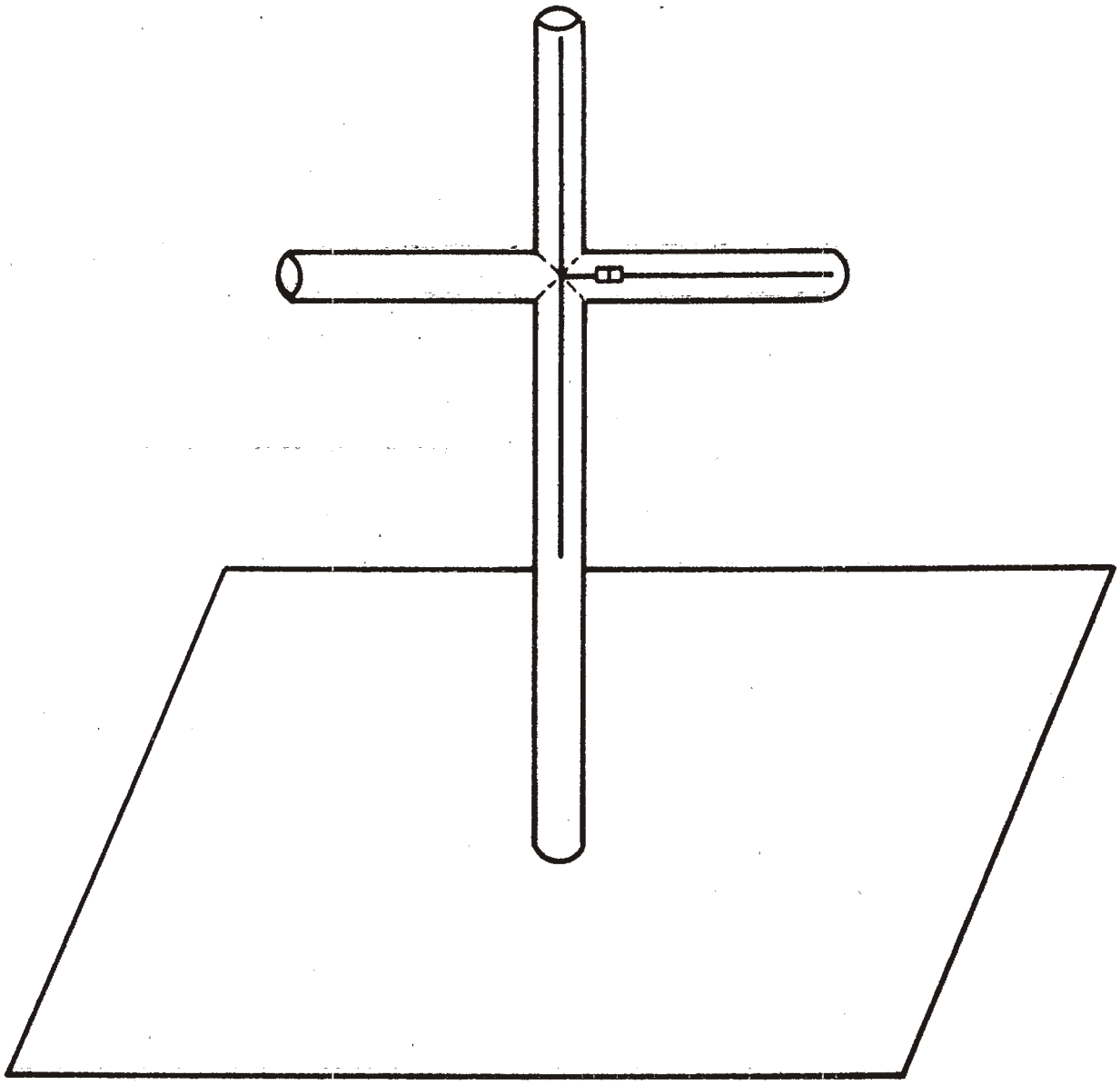

FIG. 1 CROSSED-DIPOLE ANTENNA

receiving crossed dipole, resonant coupling lengths between various cross members were examined. In particular, junction effects were investigated at current maximum/charge minimum, current minimum/charge minimum, and current minimum/charge maximum as well as one intermediate case. For polarizations other than vertical the results of this paper may be generalized through superposition and symmetry considerations.

II. Measurement of Distributions of Current and Charge Per Unit Length

The apparatus for measuring current and charge per unit length was specifically designed to study the distributions near the junction of the crossed-dipole receiving antenna. Both the parasitic monopole and the crossed dipole consisted of brass tubes slotted for internally mounted probes terminated in flat end caps and mounted vertically over a large aluminum ground plane. They were illuminated by a vertically polarized electromagnetic field generated by a driven monopole with a corner reflector nearly ten wave-lengths away so that the phase fronts of the incident waves at the receiving elements approximated a plane wave. Measurements were made at two frequencies for which the electrical radius of the antenna was $ka = 0.033$ and $ka = 0.044$ where $k = 2\pi/\lambda$ and a is the outer radius of the brass tubing.

The instrumentation consisted of a flush-mounted monopole for a charge probe and a small shielded loop as a current probe. These could be moved along the slots in the vertical and horizontal arms of the receiving antenna by an internal mechanism controlled by a rack-and-pinion positioner mounted beneath the ground plane. In order to obtain various standing-wave patterns and resonant interactions, the lengths of both vertical member and horizontal arms were varied over a wide range.

III. Description of Experimental Results for Receiving Monopole

The principal reason for examining in detail the standing-wave patterns of the induced current and charge per unit length along a conductor with the electric field parallel to its axis is to establish a physical basis of understanding for the far more complicated distributions occurring on the crossed dipole. The first parasitic or receiving monopole investigated was $3\lambda/4$ long, a length near resonance. The theoretical distributions of current and charge per unit length are shown in figure 2. Both amplitudes and phases resemble those along a resonant open-ended section of coaxial line in that the maxima of the current and the minima of the charge are virtually coincident near $kz = 0$ and π or at $\lambda/4$ and $3\lambda/4$ from the open end. Correspondingly, the minima of the current and maxima of the charge occur close together at $kz = \pi/2$ and at the open end $kz = kh = 3\pi/2$. Rapid changes in phase by 180° occur near the minima, indicating a reversal in direction of the principal components of both current and charge. While the amplitude and phase of the charge behave very closely like those in a coaxial line with an open end, there are significant differences in the distribution of current. These include a minimum that is not as sharp and deep, two maxima that differ greatly from each other in amplitude - the one at $kz = 0$ is much smaller, and a phase angle θ_I that changes only gradually through the 180°. These differences are a

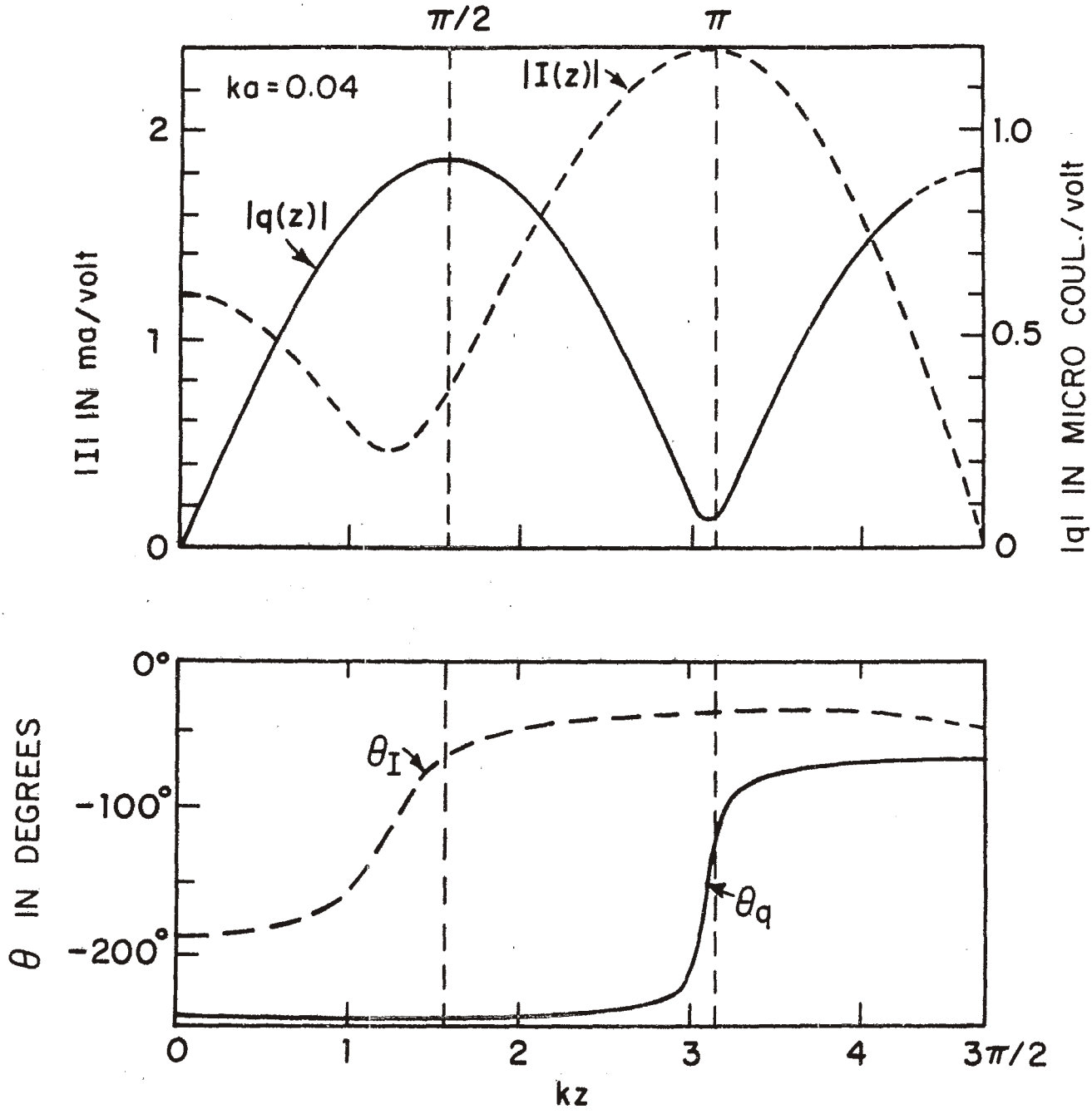

FIG. 2 THEORETICAL DISTRIBUTIONS OF CURRENT AND CHARGE IN PARASITIC MONOPOLE IN NORMALLY INCIDENT FIELD; $h = 3\lambda/4$

consequence of the continuous uniform excitation along the entire length instead of by a single localized generator. Measured curves for the same electrical length but with a slightly smaller value of ka are shown in figure 3. All four curves are seen to agree well in all significant details with the corresponding theoretical ones.

When the length of the monopole is increased to $3\lambda/2$ as shown in figure 4, the distribution of charge remains conventional in both amplitude and phase. Maxima occur at intervals of $\lambda/2$; and these are displaced by $\lambda/4$ from the minima. The phase angle θ_q changes rapidly by 180° at the minima. The distribution of current is quite different. Its maxima occur at intervals of λ, as do its minima. The phase angle θ_I is sensibly constant over the entire length of the antenna with only relatively small (compared with variations in θ_q) dips at the minima of current.

The measured curves for $h = 3\lambda/2$ are shown in figure 5. As indicated previously, measurements were designed only to be made in the junction region of the crossed dipole and were made only out a distance $kz = 3\pi/2$ from the ground plane. A comparison of figures 4 and 5 shows that the theoretical and measured magnitudes $|q(z)|$ and phase angles θ_q of the charge per unit length agree well as do the phase angles θ_I of the currents. However, whereas the theoretical current amplitude has a minimum at $kz = \pi$, the measured curve shows a peculiar minor maximum. This is not an error but is readily explained with the help of a slight increase

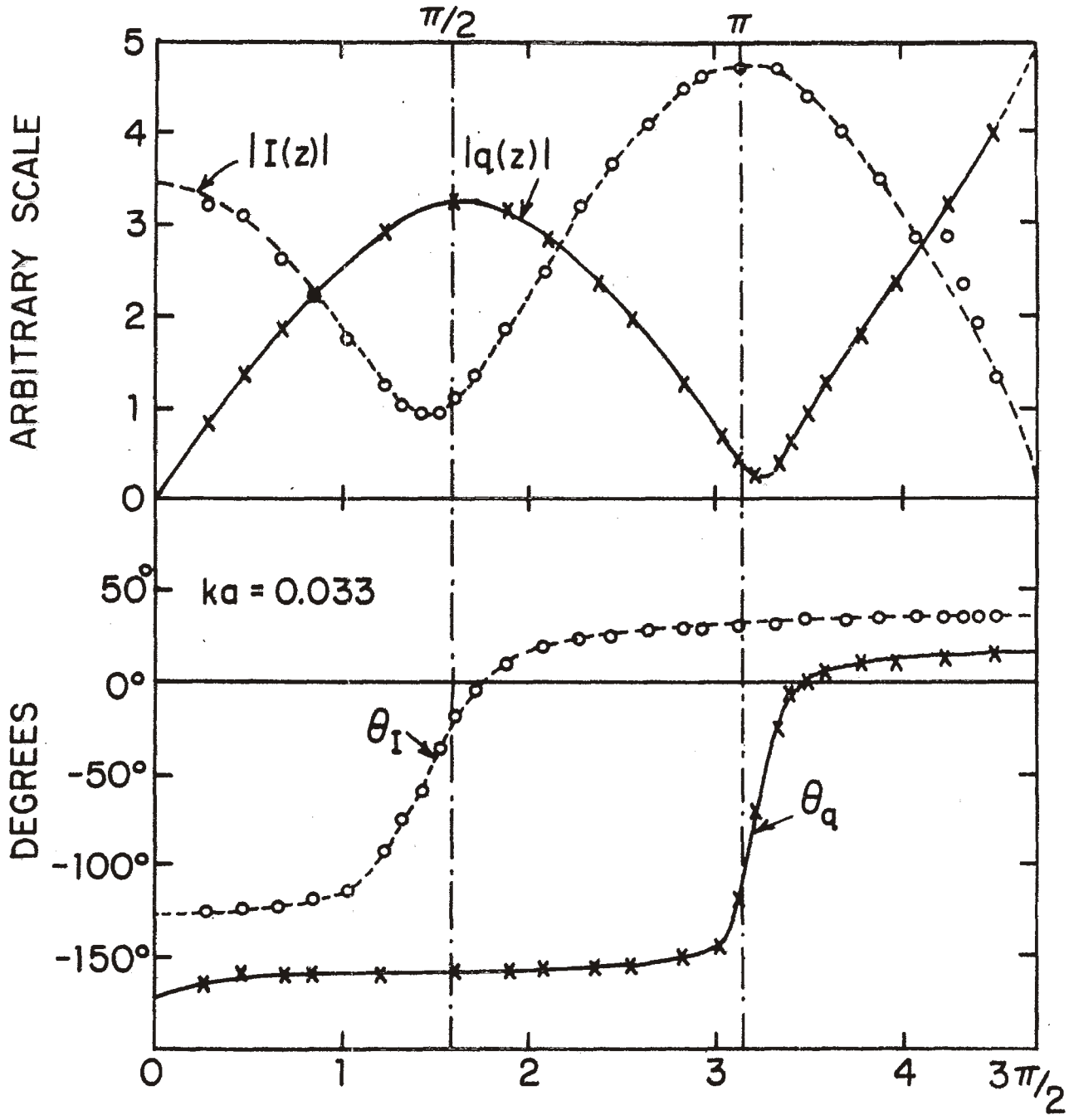

FIG. 3 MEASURED DISTRIBUTIONS OF CURRENT AND CHARGE IN PARASITIC MONOPOLE IN NORMALLY INCIDENT FIELD, $h = 3\lambda/4$

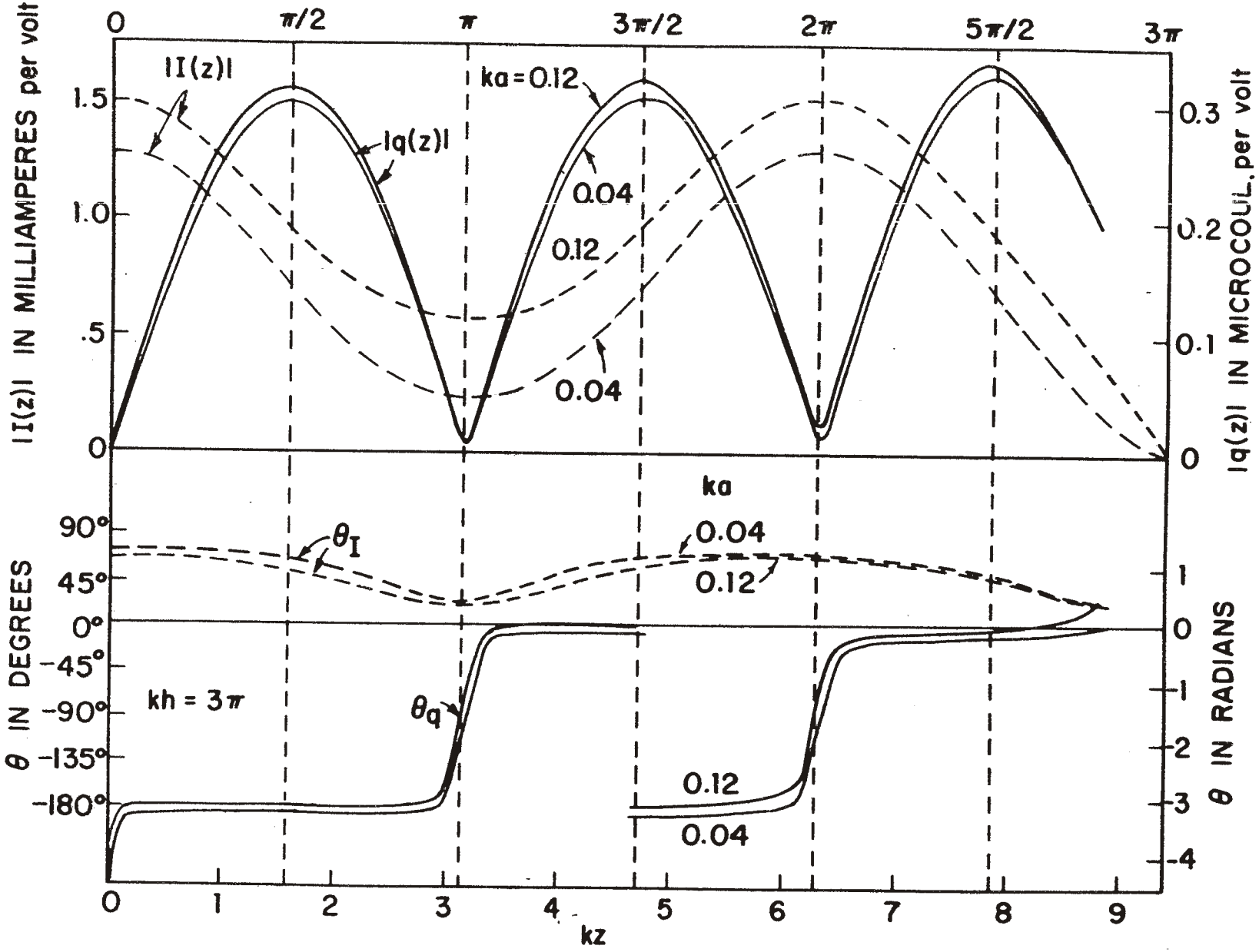

FIG. 4 THEORETICAL DISTRIBUTIONS OF CURRENT AND CHARGE IN PARASITIC ANTENNA IN NORMALLY INCIDENT FIELD, $h = 1.5\lambda$

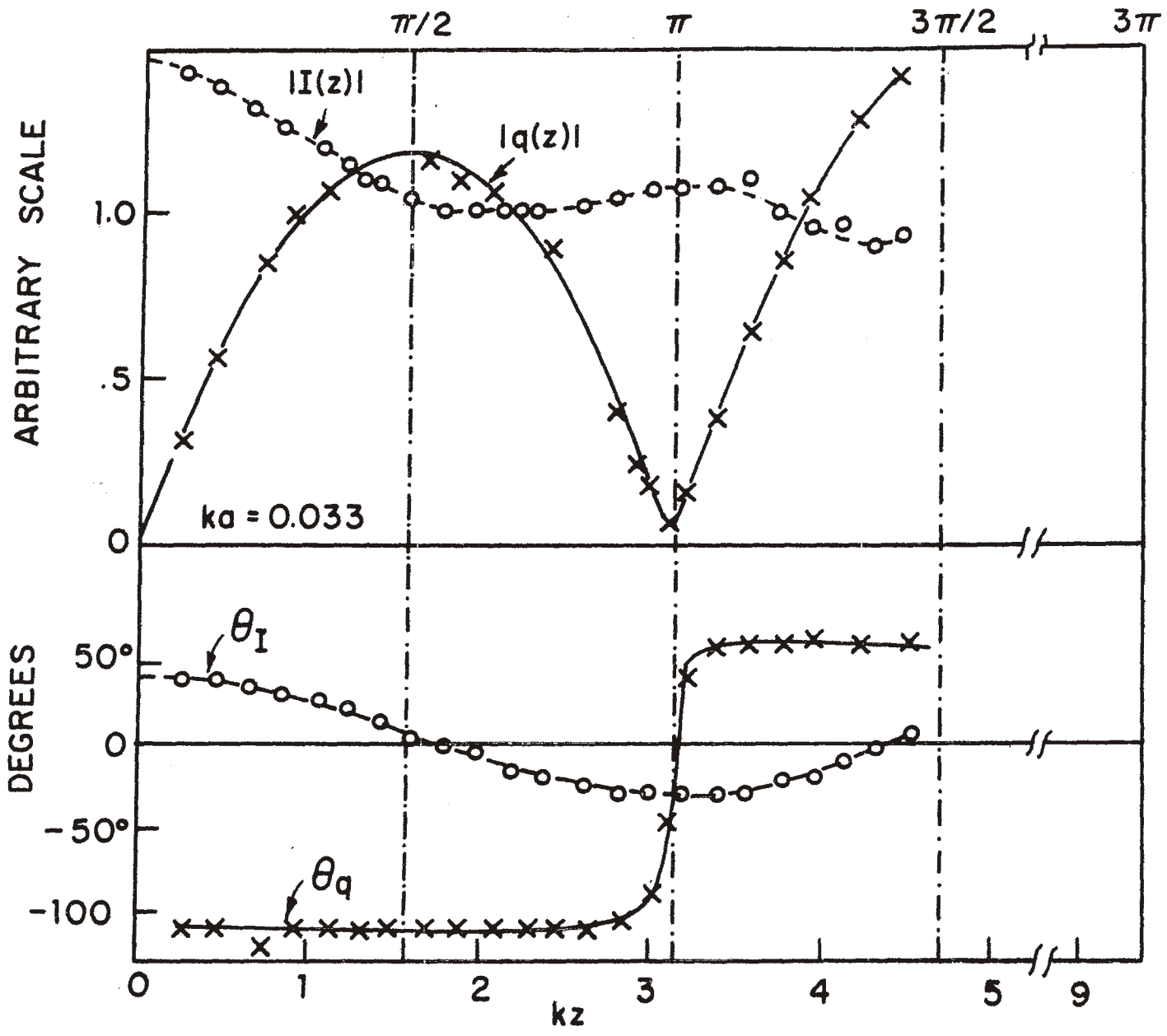

FIG. 5 MEASURED DISTRIBUTIONS OF CURRENT AND CHARGE IN PARASITIC MONOPOLE IN NORMALLY INCIDENT FIELD. $h = 1.5\lambda$.

in the length of the antenna for the theoretical calculation. Figure 6 shows the same theoretical curves but for kh = 10.2 instead of kh = 3π. The amplitude and phase angle of the charge and the phase angle of the current show little change. But, a minor maximum now occurs at kz = π in the graph for $|I(z)|$ in close correspondence with the measured curve in figure 5. Actually, this minor maximum is considerably greater than the measured one, indicating that an even smaller increase in length would have sufficed. Thus, it is seen that the standing-wave pattern of current can be very sensitive to the length of the antenna.

The final example of the distributions of current and charge per unit length is for a near resonant length with h = $5\lambda/4$, a half-wavelength longer in half-length than used in figure 2. In this case the charge distribution once again looks conventional with maxima at intervals of a half-wavelength and 180° changes in the phase angle as the amplitude goes through a minimum. A zero of charge per unit length is at the ground plane, a maximum at the open end. The current has maxima at the minima of charge, but whereas the maxima at kz = 0 and kz = 2π are almost equal in magnitude and quite large, that at kz = π is much smaller. Furthermore, the phase angle θ_I has equal values near kz = 0 and kz = 2π, but quite a different range of values near kz = π. Measured curves for an antenna of length kh = $5\pi/2$ are shown in figure 7. The theoretical and measured distributions of both amplitudes and phase angles are very much alike.

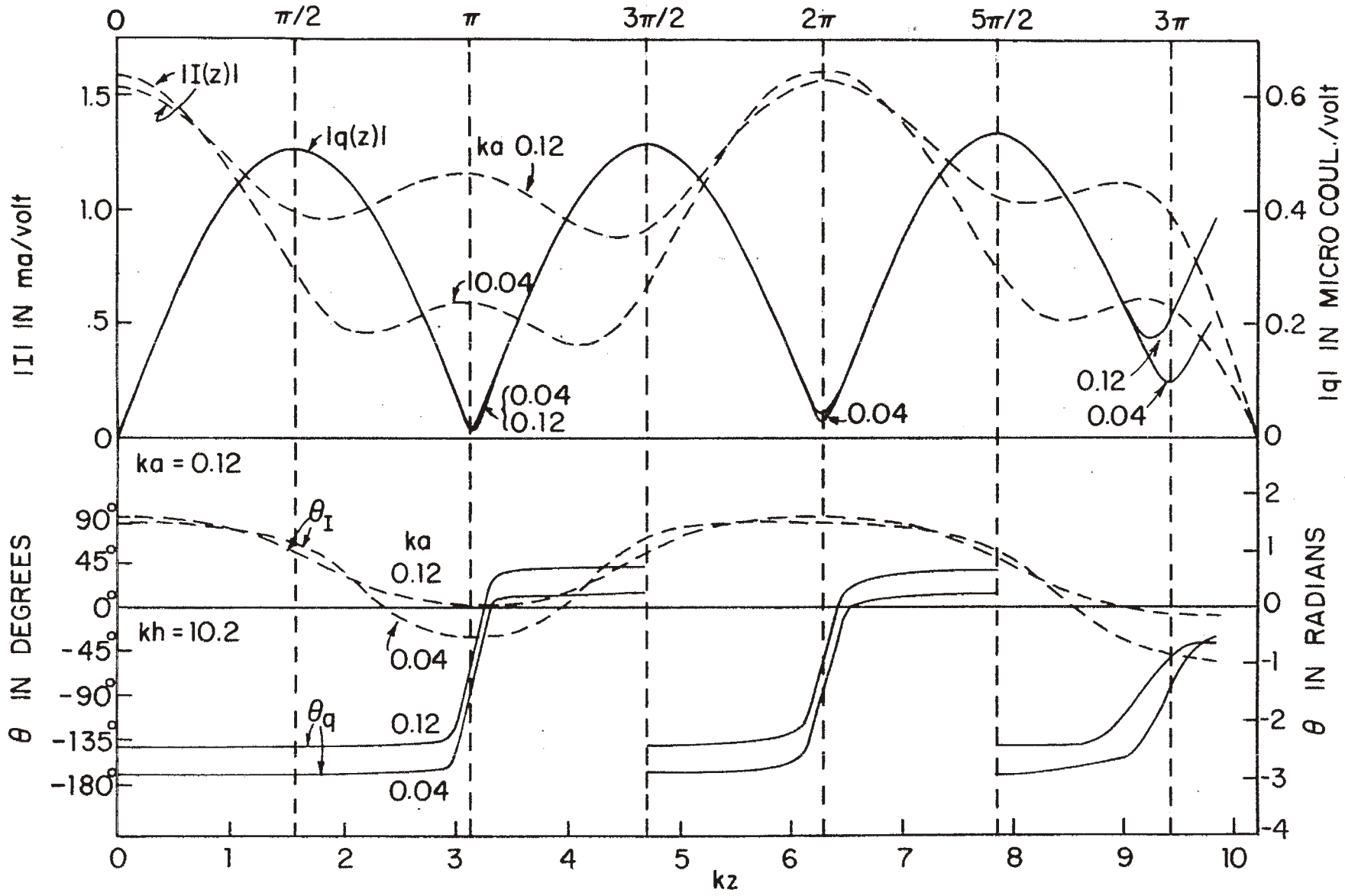

FIG. 6 THEORETICAL DISTRIBUTIONS OF CURRENT AND CHARGE PER UNIT LENGTH IN PARASITIC ANTENNA IN NORMALLY INCIDENT FIELD, h=1.62 λ

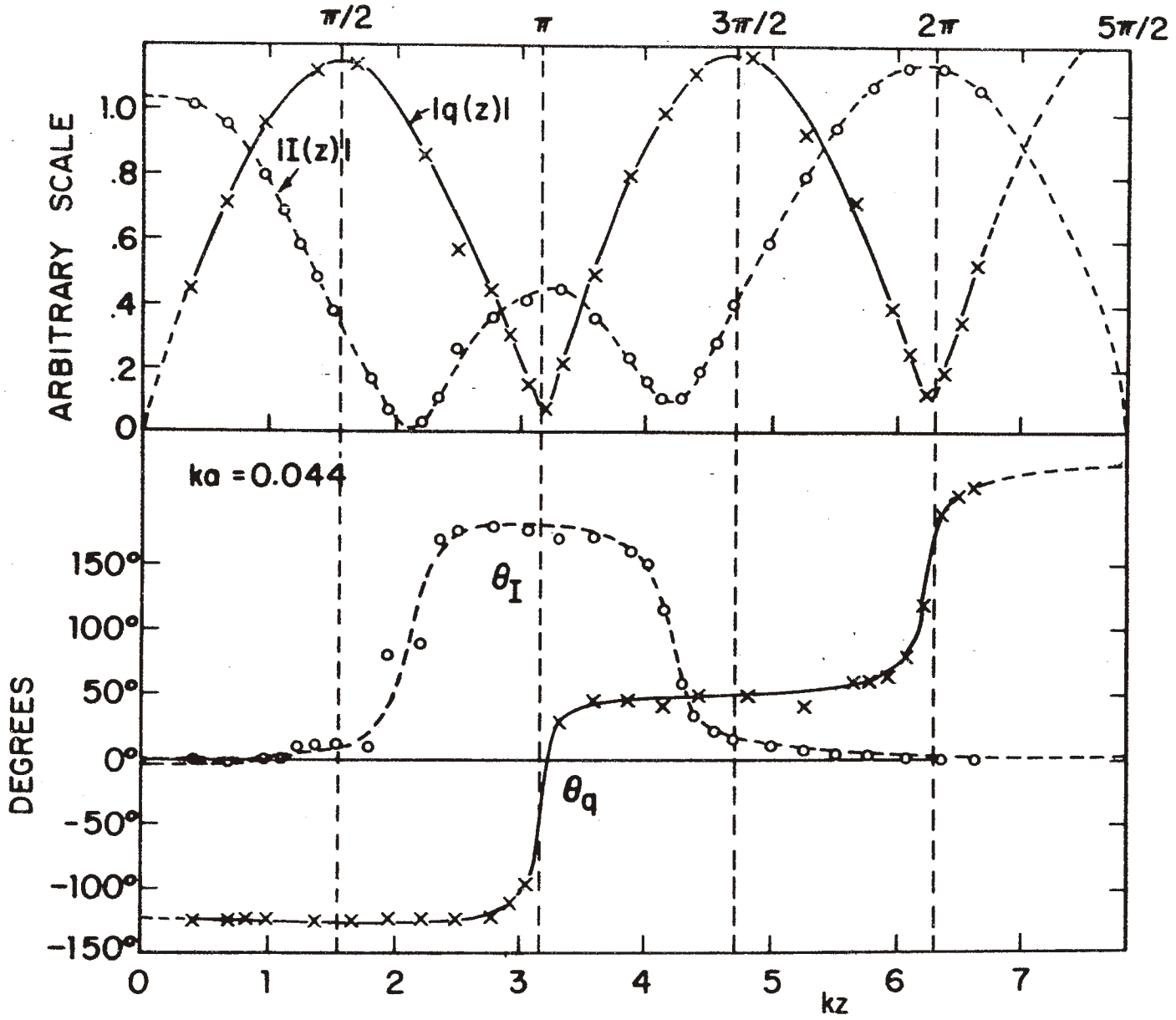

FIG. 7 MEASURED DISTRIBUTIONS OF CURRENT AND CHARGE PER UNIT LENGTH IN PARASITIC MONOPOLE $h = 5\lambda/4$

A study of the several distribution curves in figures 2 through 7 shows that the charge per unit length behaves in a very simple and predictable manner. In a zero-order approximation it is given by

$$q(z) \sim \sin kz \qquad (1)$$

At the base of a monopole or the center of a dipole the charge per unit length must vanish to satisfy the symmetry condition $q(-z) = -q(z)$. All of the graphs of $q(z)$ are quite well approximated by the simple form (Eq. 1) except for the occurrence of deep minima instead of nulls which are accounted for by higher-order terms.

In order to understand the peculiarities in the standing-wave patterns of current, it is advantageous to examine the behavior of the components of the induced currents that are in phase and in phase quadrature with the incident field. A complete discussion of this aspect as well as a thorough analysis of the parasitic monopole is presented by King and this author (Burton, R. W. and King, R. W. P., to be published).

The principal reason for examining in detail the standing-wave patterns of the induced current and charge per unit length of the receiving monopole was to establish a physical basis of understanding for the much more complicated distributions which result from a second conductor being connected perpendicular to the first. The coupling of this horizontal element which would have otherwise been

completely uncoupled from the vertically polarized incident field before the connection was made is determined in part by the currents and charges present at the proposed junction region of the receiving monopole and, as will be described later, by the various combinations of resonant lengths which result from the connection.

IV. Description of Experimental Results for Receiving Crossed Dipole

With the use of Eq. 1 and the shifted cosine distribution for current (King, R. W. P., 1956), a number of special cases can readily be constructed which give insight into conditions in the junction region (figure 8). The horizontal mark on each of the cases in figure 8 locates the proposed junction location for the horizontal cross arm. It is clear that if a horizontal cross arm is located at $h = \lambda/2$ above the ground plane, junction effects may be studied for perturbations in an area of current maximum and charge minimum on the vertical member as in Cases 1 and 2, and current minimum/charge minimum in Case 3. Similarly, if the cross arm is located at $h = 3\lambda/4$, junction effects may be investigated for a condition of current minimum and charge maximum as in Cases 4 and 5. Case 6 is an intermediate case and is included to examine the situation when there is both charge and current present in the junction region. In order to shift the junction from $h = \lambda/2$ to $h = 3\lambda/4$, the frequency of the incident plane wave was merely changed by the appropriate amount, which of course causes a shift of ka. To summarize, for the cases where the cross arms are located at $h = \lambda/2$, $ka = 0.044$; when they are located at $h = 3\lambda/4$, $ka = 0.033$.

A vertically polarized incident wave will clearly not excite longitudinal currents along the axis of a dipole located horizontally and parallel to the plane-wave front.

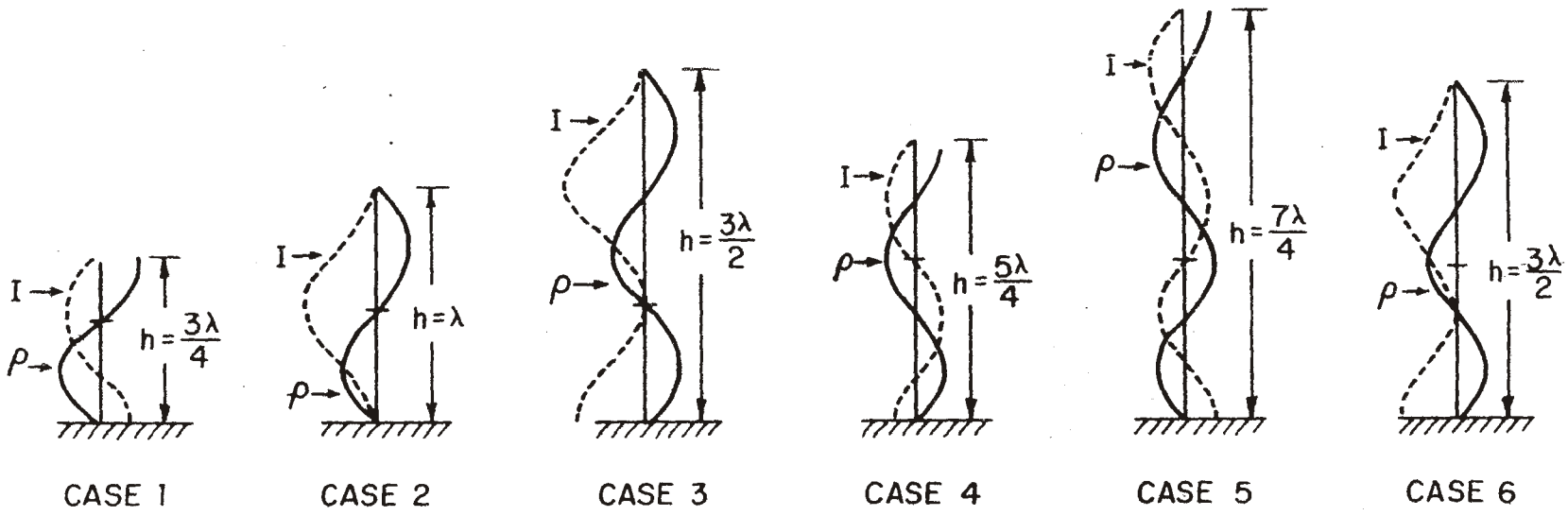

CHARGE AND CURRENT DENSITY ON DIPOLE RECEIVING ANTENNA MOUNTED OVER CONDUCTING GROUND PLANE AS A FUNCTION OF ANTENNA LENGTH (h)

FIGURE 8

However, when the horizontal and vertical dipoles are joined together, significant charge and current densities are observed along the horizontal member at various combinations of resonant lengths. A resonant length for the crossed dipole is considered to be any length measured through the junction involving any two of the four arms which gives rise to resonant effects.

When the horizontal dipole is joined to the vertical dipole, it is useful for physical insight to consider the vertical receiving dipole (which is coupled to the incident vertically polarized wave) as driving the otherwise uncoupled horizontal member through the interaction of the charges and currents present in the junction region. The amount of coupling is essentially determined by the various possibly resonant lengths as measured through the junction.

The addition to the vertical dipole of the horizontal cross member can best be regarded as loading the junction, whereas the cross member becomes an antisymmetrically driven antenna. The drive comes about from the source currents and charges existing in the junction region. When the horizontal member is added these source currents and charges spread out onto the cross arm, thereby causing an observable dip in the charge and current distributions as measured along the vertical member. The currents and charges on a driven antenna may be separated (King, R. W. P., 1956) into symmetrical and antisymmetrical components (figure 9). In the case of the horizontal cross member of the crossed

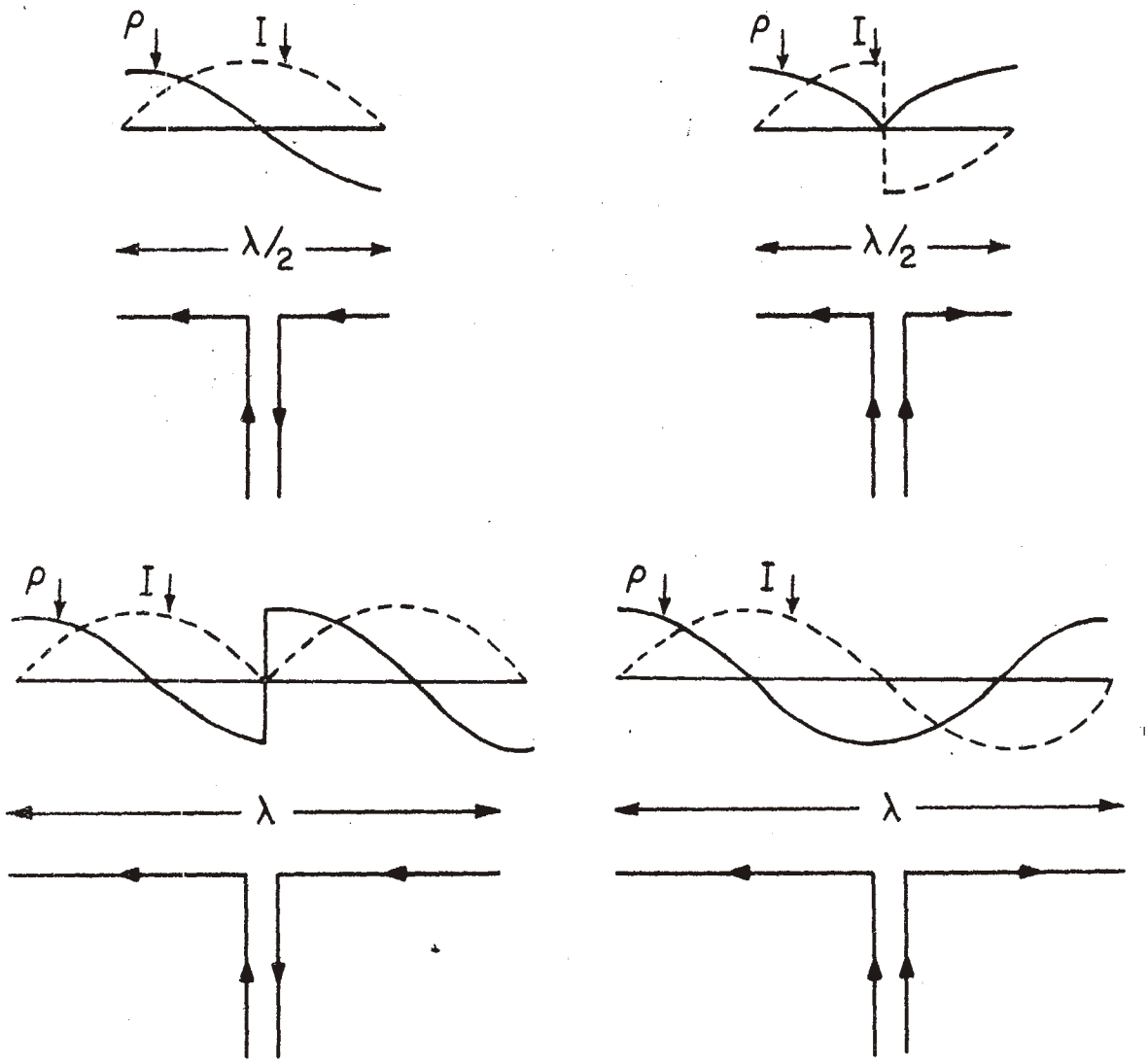

CURRENT AND CHARGE DENSITY ON SYMMETRICAL AND ANTISYMMETRICAL DRIVEN ANTENNAS

FIGURE 9

dipole under investigation, the currents on the vertical dipole branch out in the junction region onto the cross arms and drive the horizontal member antisymmetrically. From another point of view the distribution patterns of currents and charges are the result of a superposition of resonant and forced distributions.

For the moderately thick dipole (Kao, C. C., 1969), Kao has shown that transverse currents exist only near the ends. It, therefore, follows that for the crossed dipole under study with symmetrical arms the only transverse currents present in the junction region will be symmetrical transverse currents branching out from the centerline to the horizontal arms, given that the junction is reasonably far (i.e., $<\lambda/4$) from the end caps. It should be noted that the use of a rotatable current probe verified this fact on a somewhat fatter model than the crossed dipole described here.

The perturbations of the charge and current density on a vertical receiving monopole which result from the addition of horizontal cross arms of various lengths were investigated for each of the six cases described in figure 8. Likewise, the charge and current densities along the horizontal arms which were associated with these perturbations were measured out to a distance $\gtrsim\lambda/4$ from the center of the junction. These results are summarized in figures 10 through 22.

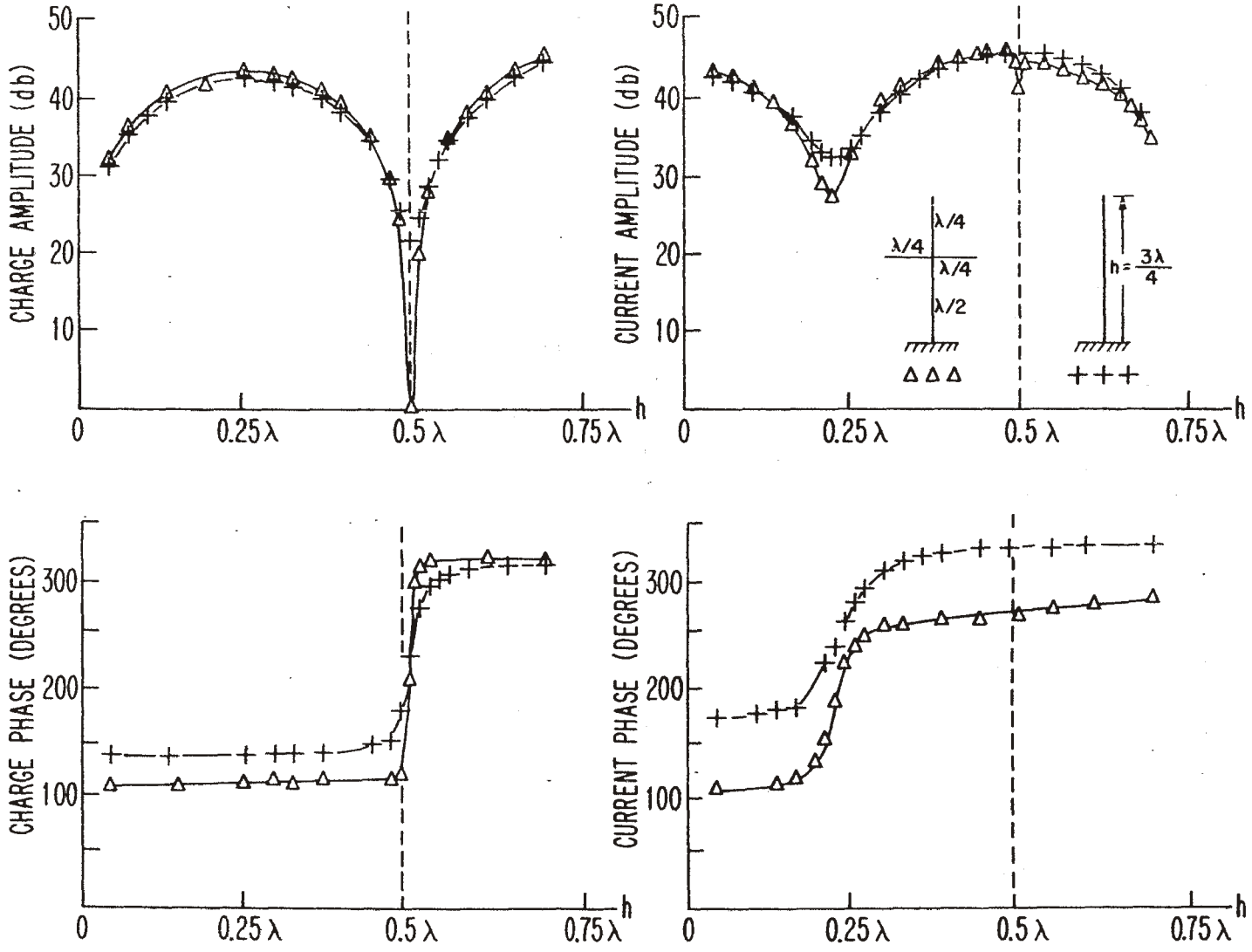

AMPLITUDE AND PHASE DISTRIBUTIONS OF CHARGE AND LONGITUDINAL CURRENT DENSITY ON VERTICAL DIPOLE AND CROSS DIPOLE ILLUMINATED BY A VERTICALLY POLARIZED PLANE WAVE AS A FUNCTION OF ANTENNA HEIGHT (h). (CASE 1)

FIGURE 10

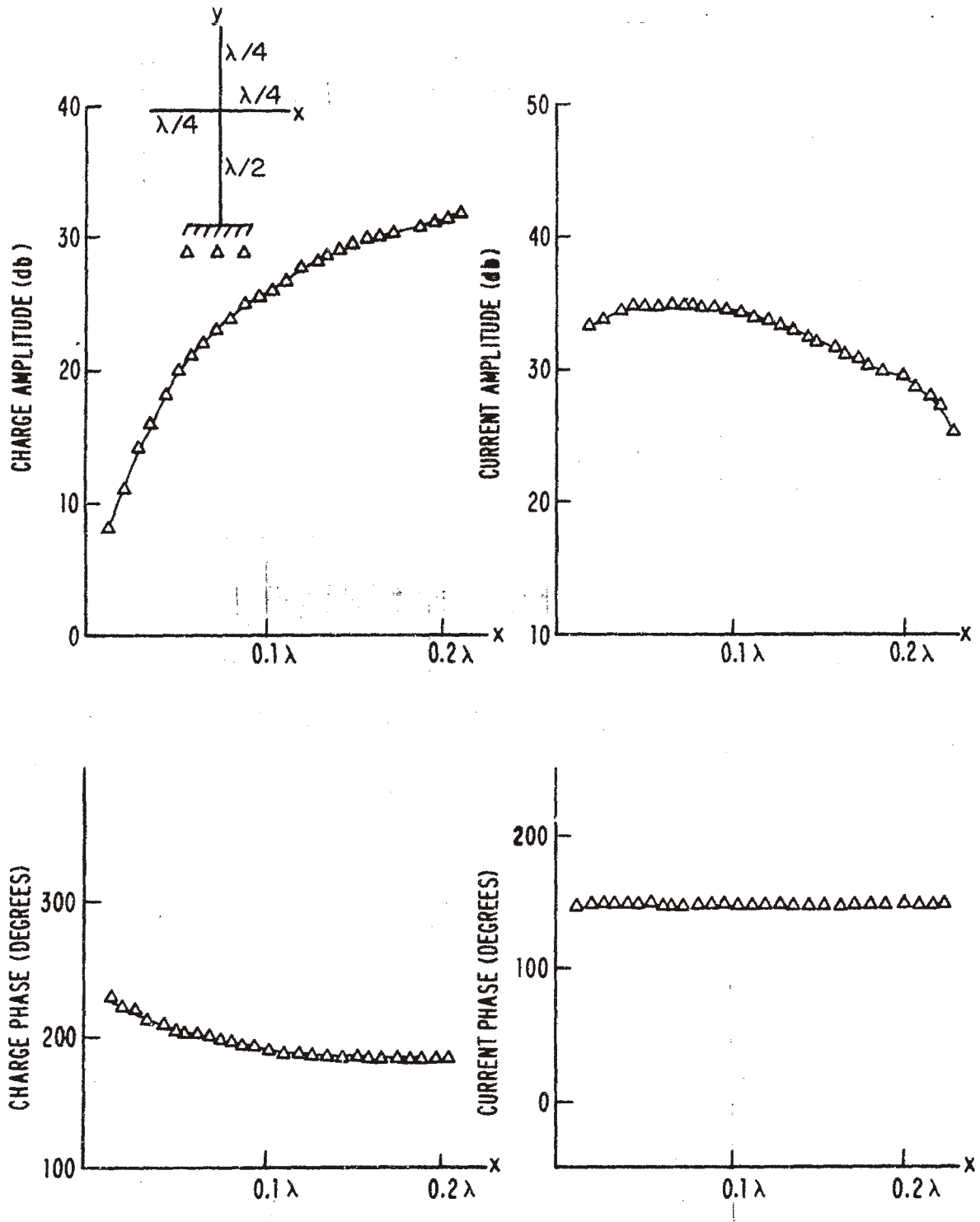

AMPLITUDE AND PHASE DISTRIBUTIONS OF CHARGE AND LONGITUDINAL CURRENT DENSITY ON HORIZONTAL ELEMENT OF CROSS DIPOLE RECEIVING ANTENNA ILLUMINATED BY A VERTICALLY POLARIZED PLANE WAVE AS A FUNCTION OF DISTANCE (WAVELENGTHS) MEASURED FROM JUNCTION. (CASE 1)

FIGURE 11

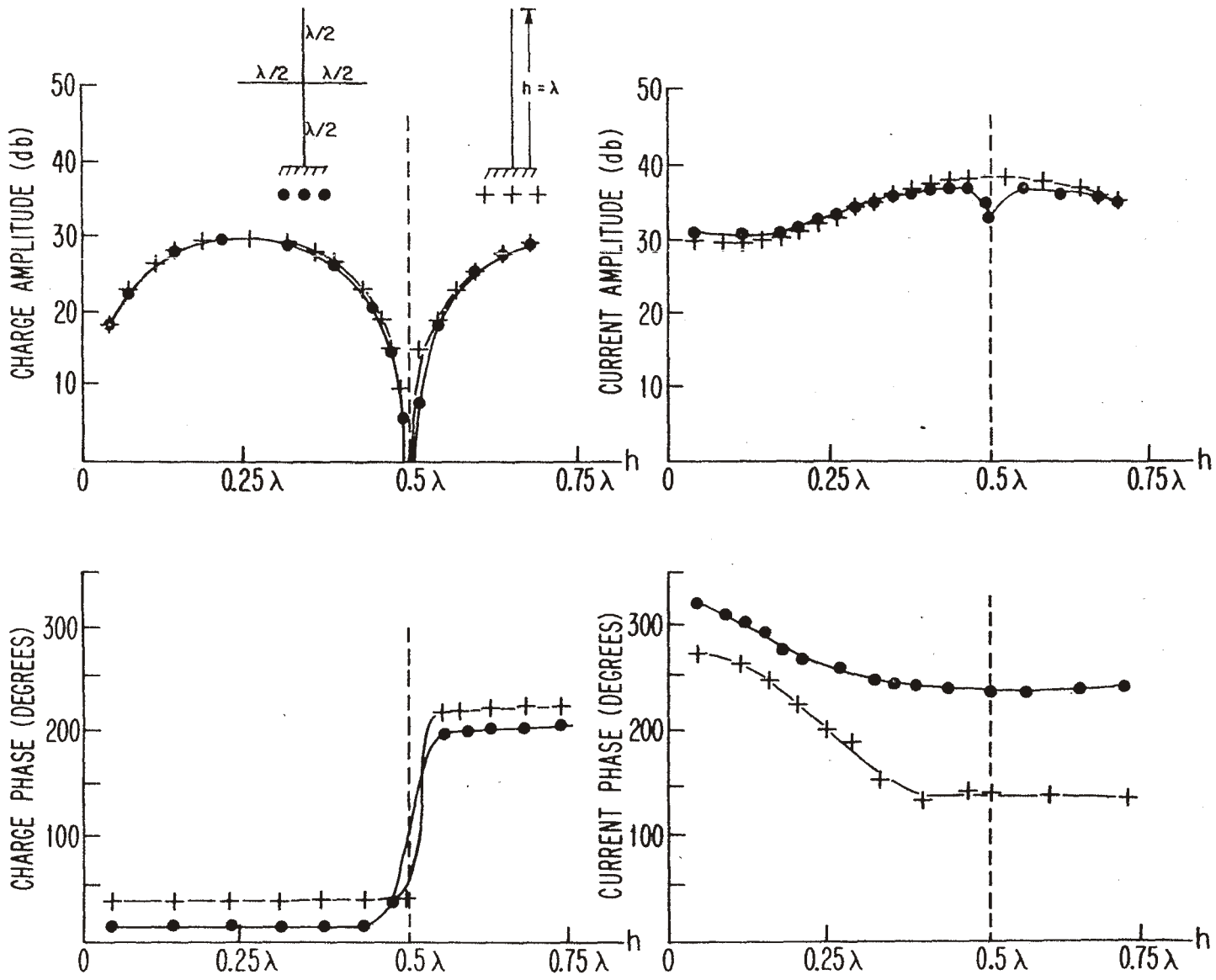

AMPLITUDE AND PHASE DISTRIBUTIONS OF CHARGE AND LONGITUDINAL CURRENT DENSITY ON VERTICAL DIPOLE AND CROSS DIPOLE ILLUMINATED BY A VERTICALLY POLARIZED PLANE WAVE AS A FUNCTION OF ANTENNA HEIGHT (h). (CASE 2)

FIGURE 12

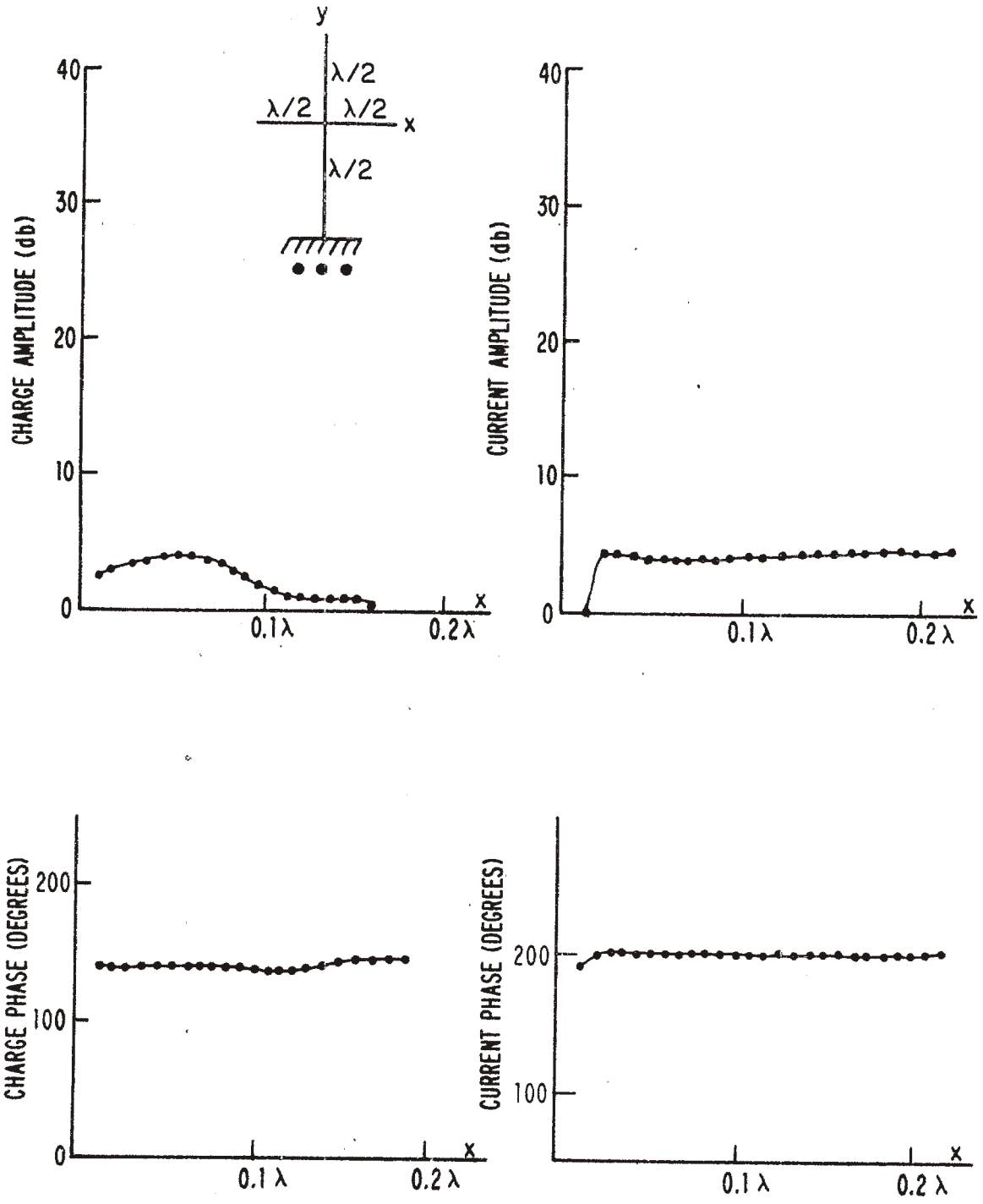

AMPLITUDE AND PHASE DISTRIBUTIONS OF CHARGE AND LONGITUDINAL CURRENT DENSITY ON HORIZONTAL ELEMENT OF CROSS DIPOLE RECEIVING ANTENNA ILLUMINATED BY A VERTICALLY POLARIZED PLANE WAVE AS A FUNCTION OF DISTANCE (WAVELENGTHS) MEASURED FROM JUNCTION. (CASE 2)

FIGURE 13

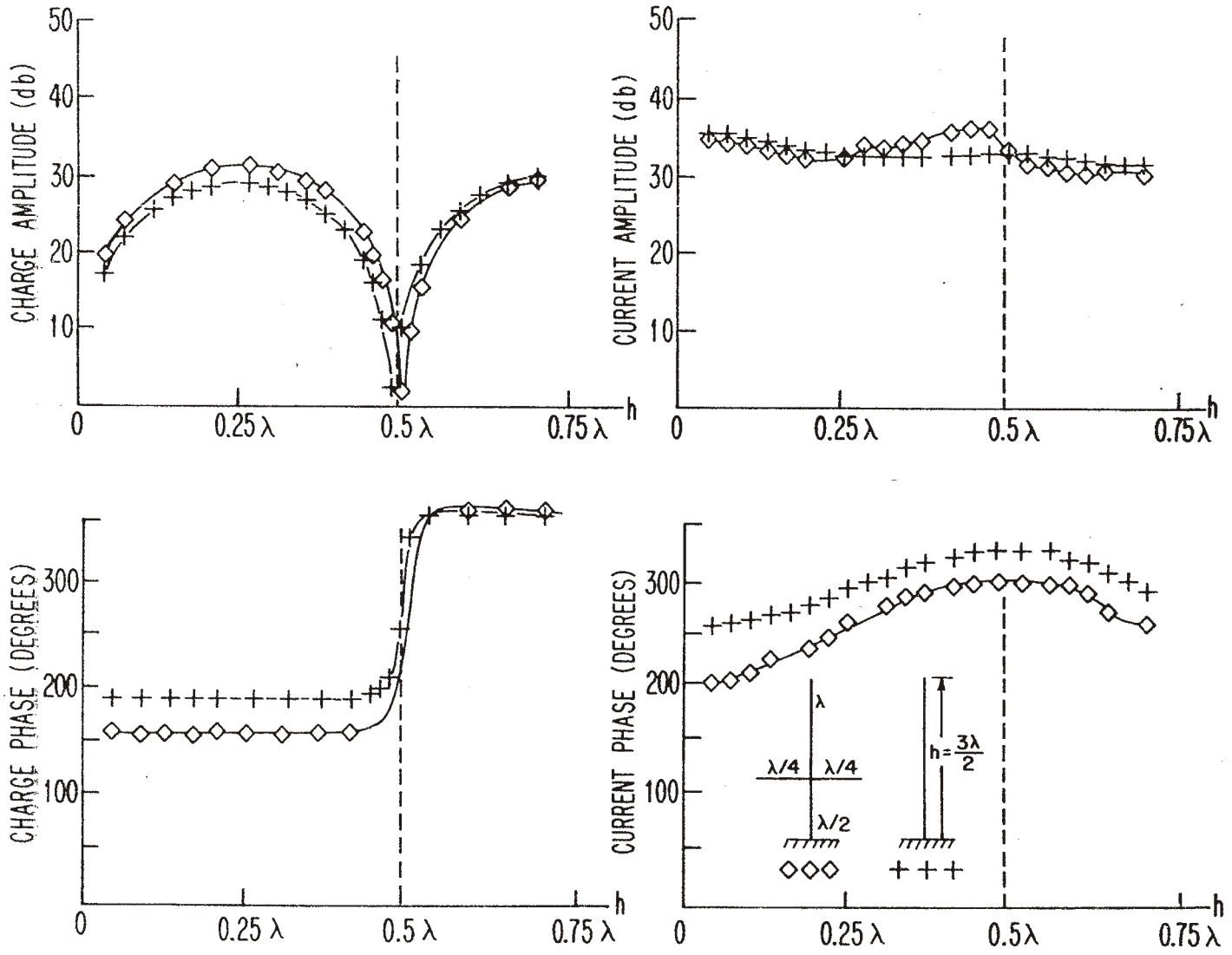

AMPLITUDE AND PHASE DISTRIBUTIONS OF CHARGE AND LONGITUDINAL CURRENT DENSITY ON VERTICAL DIPOLE AND CROSS DIPOLE ILLUMINATED BY A VERTICALLY POLARIZED PLANE WAVE AS A FUNCTION OF ANTENNA HEIGHT (h). (CASE 3)

FIGURE 14

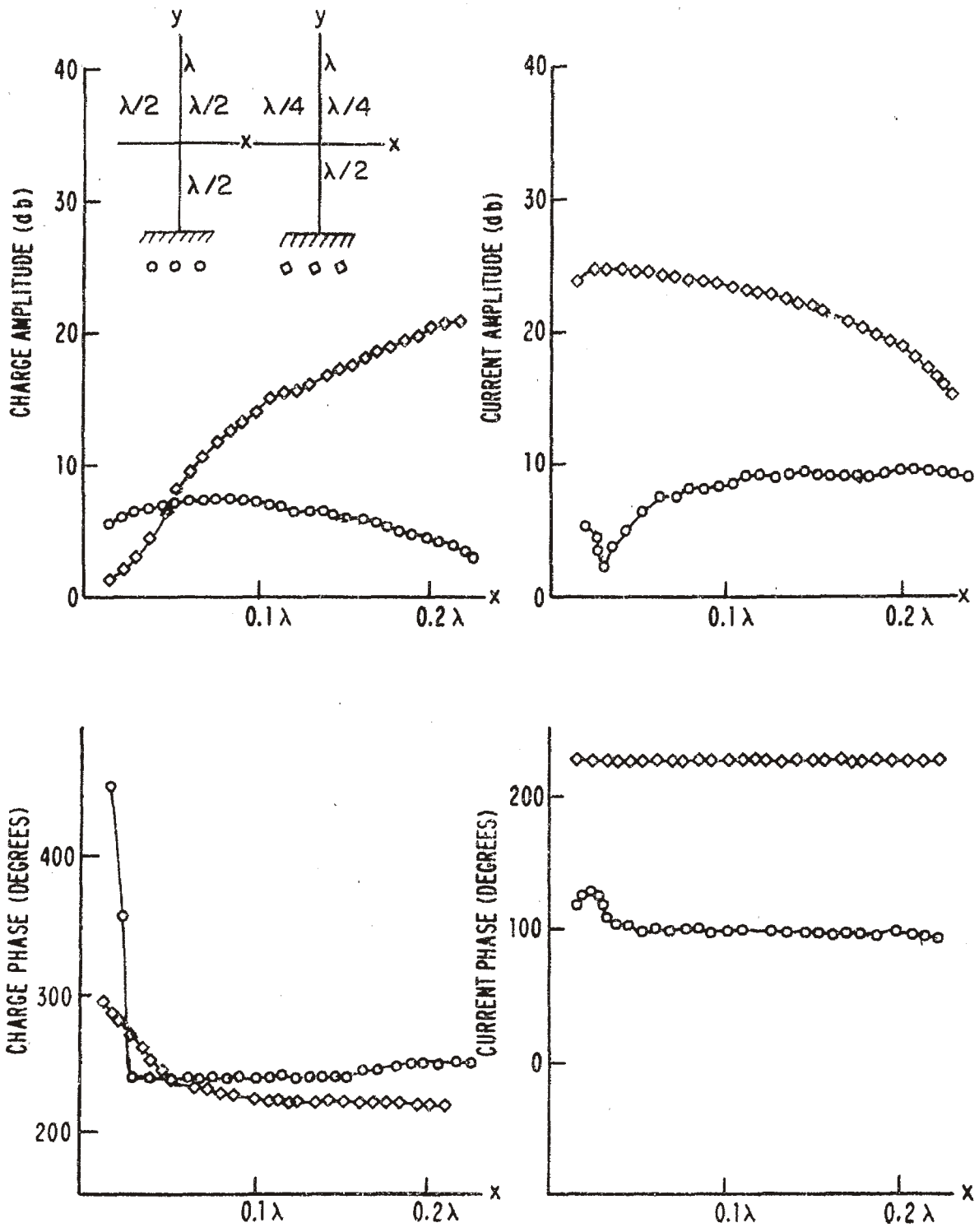

AMPLITUDE AND PHASE DISTRIBUTIONS OF CHARGE AND LONGITUDINAL CURRENT DENSITY ON HORIZONTAL ELEMENT OF CROSS DIPOLE RECEIVING ANTENNA ILLUMINATED BY A VERTICALLY POLARIZED PLANE WAVE AS A FUNCTION OF DISTANCE (WAVELENGTHS) MEASURED FROM JUNCTION. (CASE 3)

FIGURE 15

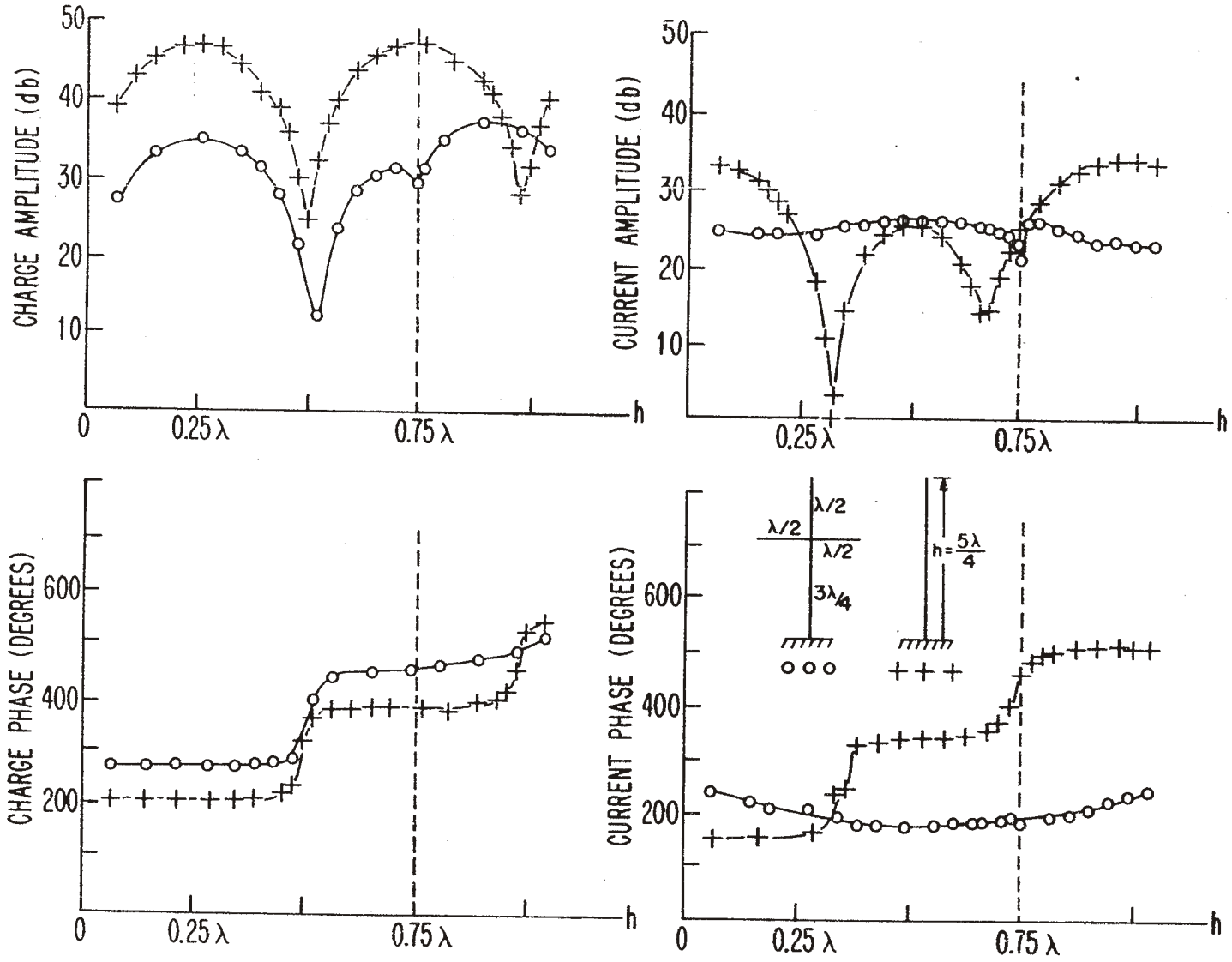

AMPLITUDE AND PHASE DISTRIBUTIONS OF CHARGE AND LONGITUDINAL CURRENT DENSITY ON VERTICAL DIPOLE AND CROSS DIPOLE ILLUMINATED BY A VERTICALLY POLARIZED PLANE WAVE AS A FUNCTION OF ANTENNA HEIGHT (h). (CASE 4)

FIGURE 16

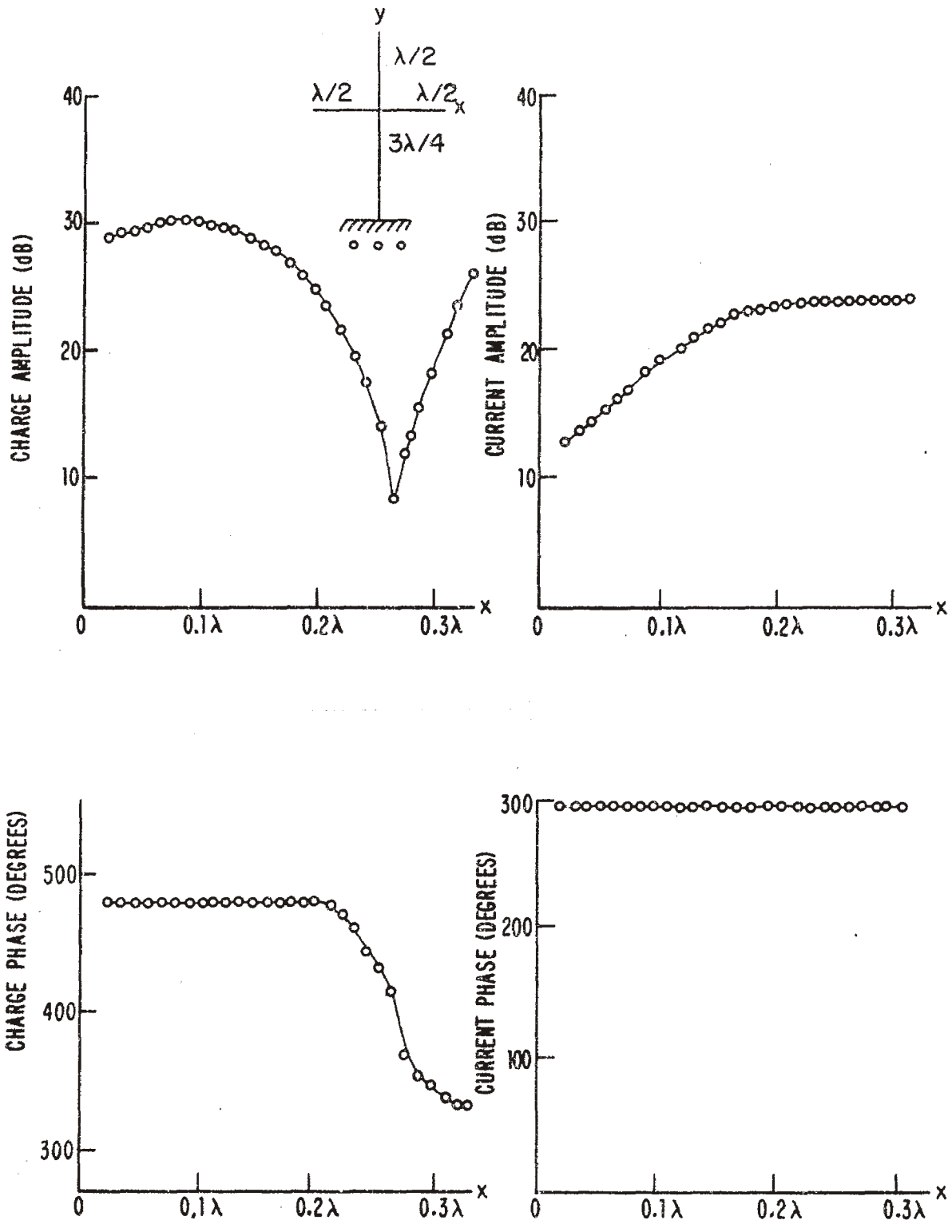

AMPLITUDE AND PHASE DISTRIBUTIONS OF CHARGE AND LONGITUDINAL CURRENT DENSITY ON HORIZONTAL ELEMENT OF CROSS DIPOLE RECEIVING ANTENNA ILLUMINATED BY A VERTICALLY POLARIZED PLANE WAVE AS A FUNCTION OF DISTANCE (WAVELENGTHS) MEASURED FROM JUNCTION. (CASE 4)

FIGURE 17

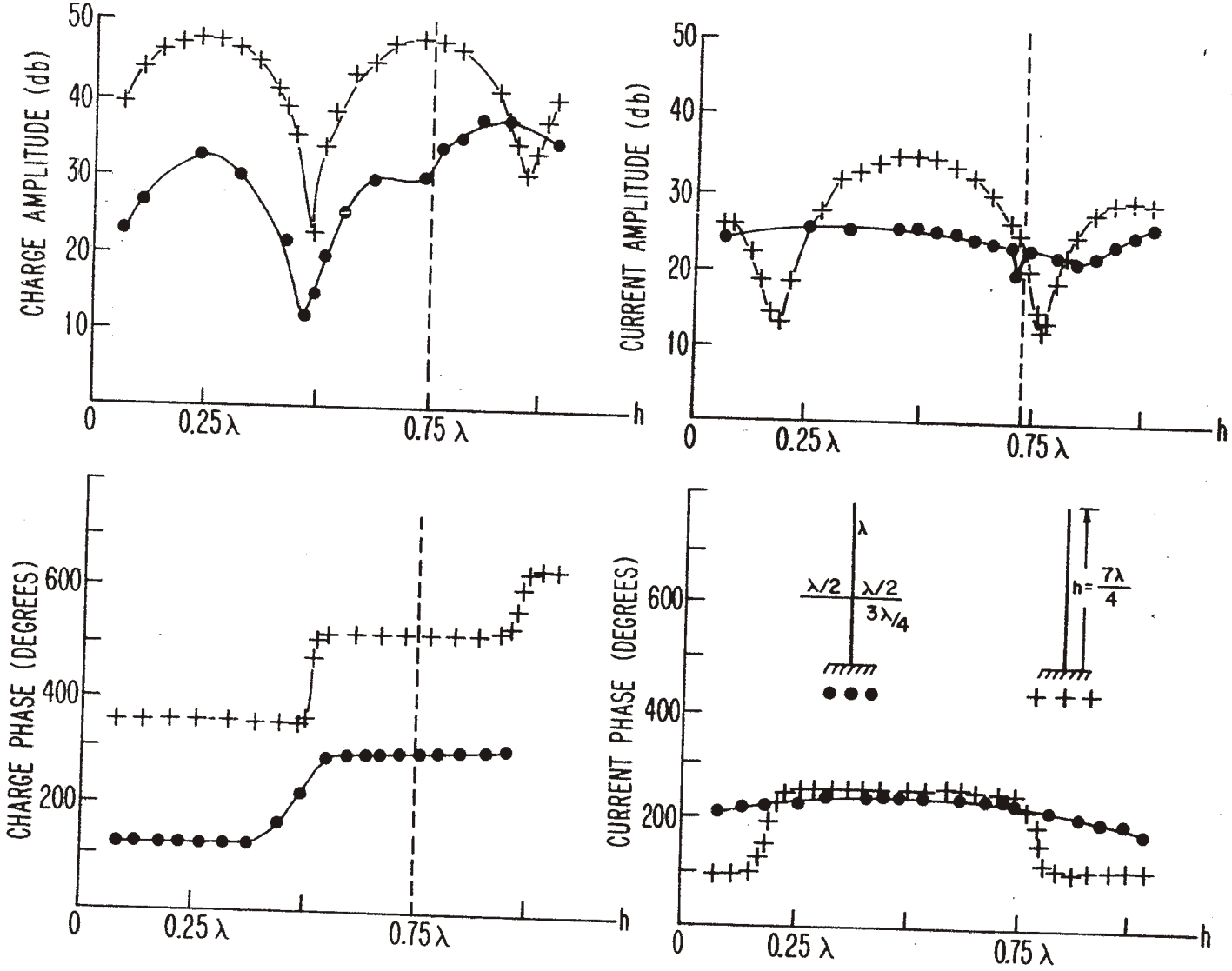

AMPLITUDE AND PHASE DISTRIBUTIONS OF CHARGE AND LONGITUDINAL CURRENT DENSITY ON VERTICAL DIPOLE AND CROSS DIPOLE ILLUMINATED BY A VERTICALLY POLARIZED PLANE WAVE AS A FUNCTION OF ANTENNA HEIGHT (h). (CASE 5)

FIGURE 18

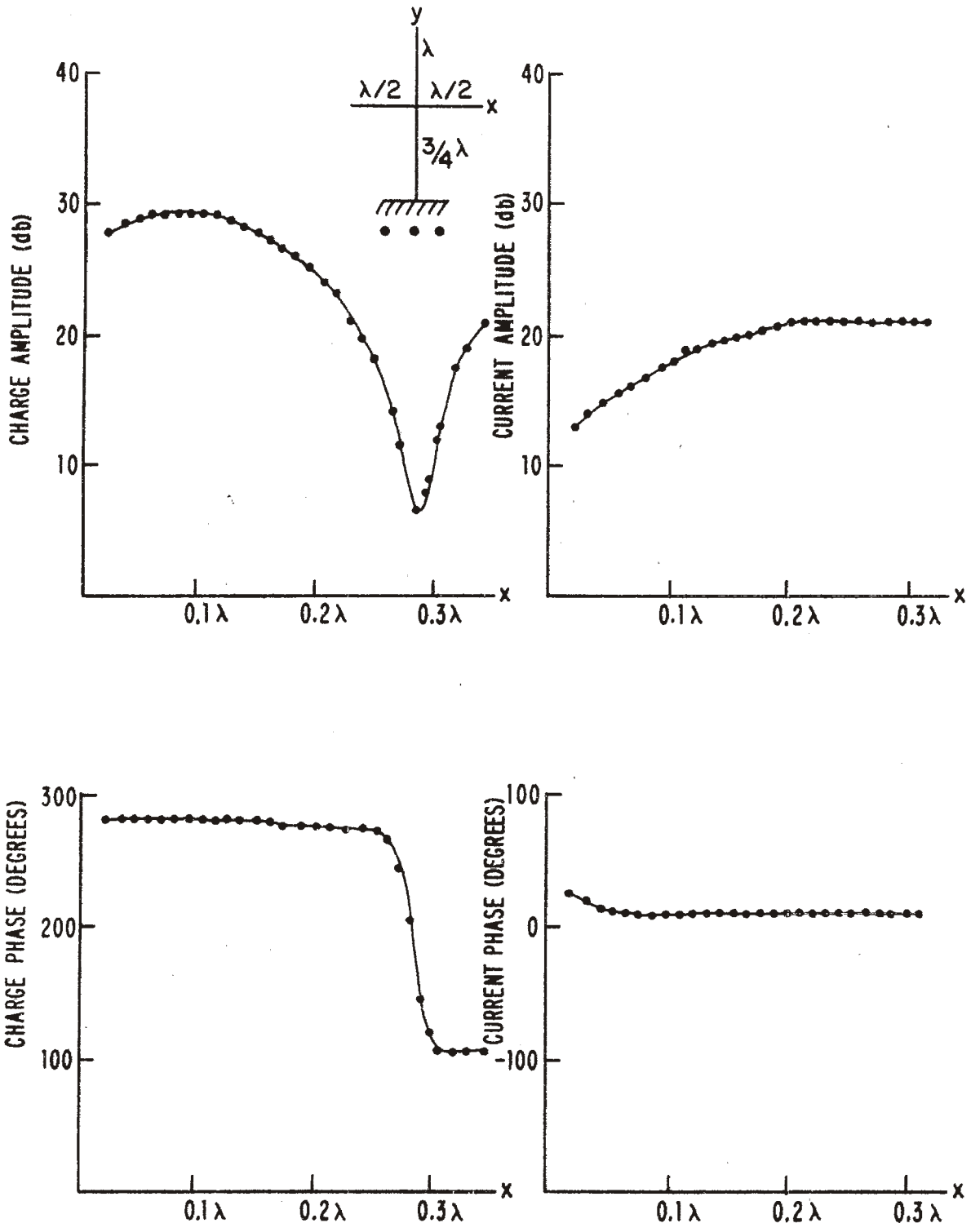

AMPLITUDE AND PHASE DISTRIBUTIONS OF CHARGE AND LONGITUDINAL CURRENT DENSITY ON HORIZONTAL ELEMENT OF CROSS DIPOLE RECEIVING ANTENNA ILLUMINATED BY A VERTICALLY POLARIZED PLANE WAVE AS A FUNCTION OF DISTANCE (WAVELENGTHS) MEASURED FROM JUNCTION. (CASE 5)

FIGURE 19

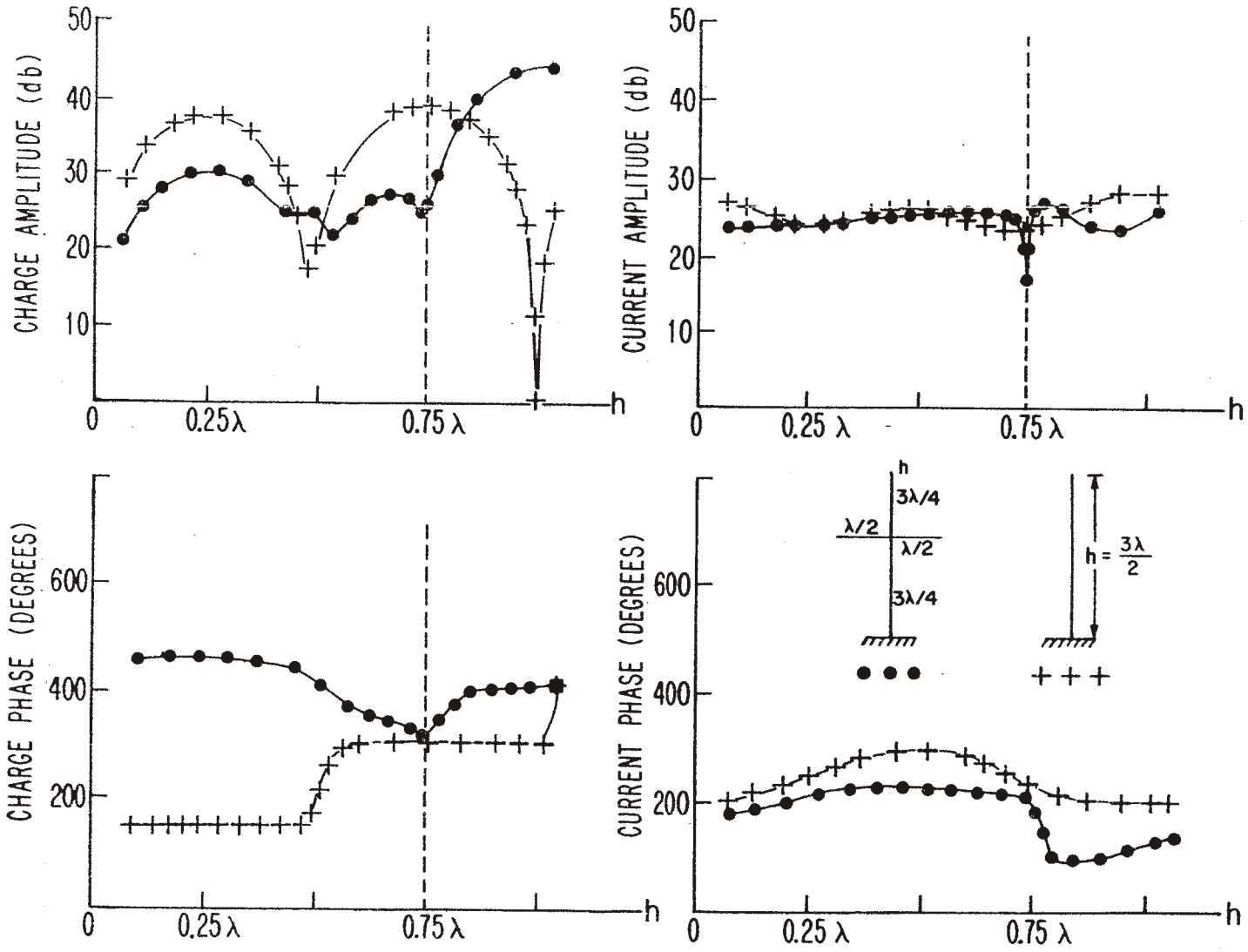

AMPLITUDE AND PHASE DISTRIBUTIONS OF CHARGE AND LONGITUDINAL CURRENT DENSITY ON VERTICAL DIPOLE AND CROSS DIPOLE ILLUMINATED BY A VERTICALLY POLARIZED PLANE WAVE AS A FUNCTION OF ANTENNA HEIGHT (h). (CASE 6)

FIGURE 20

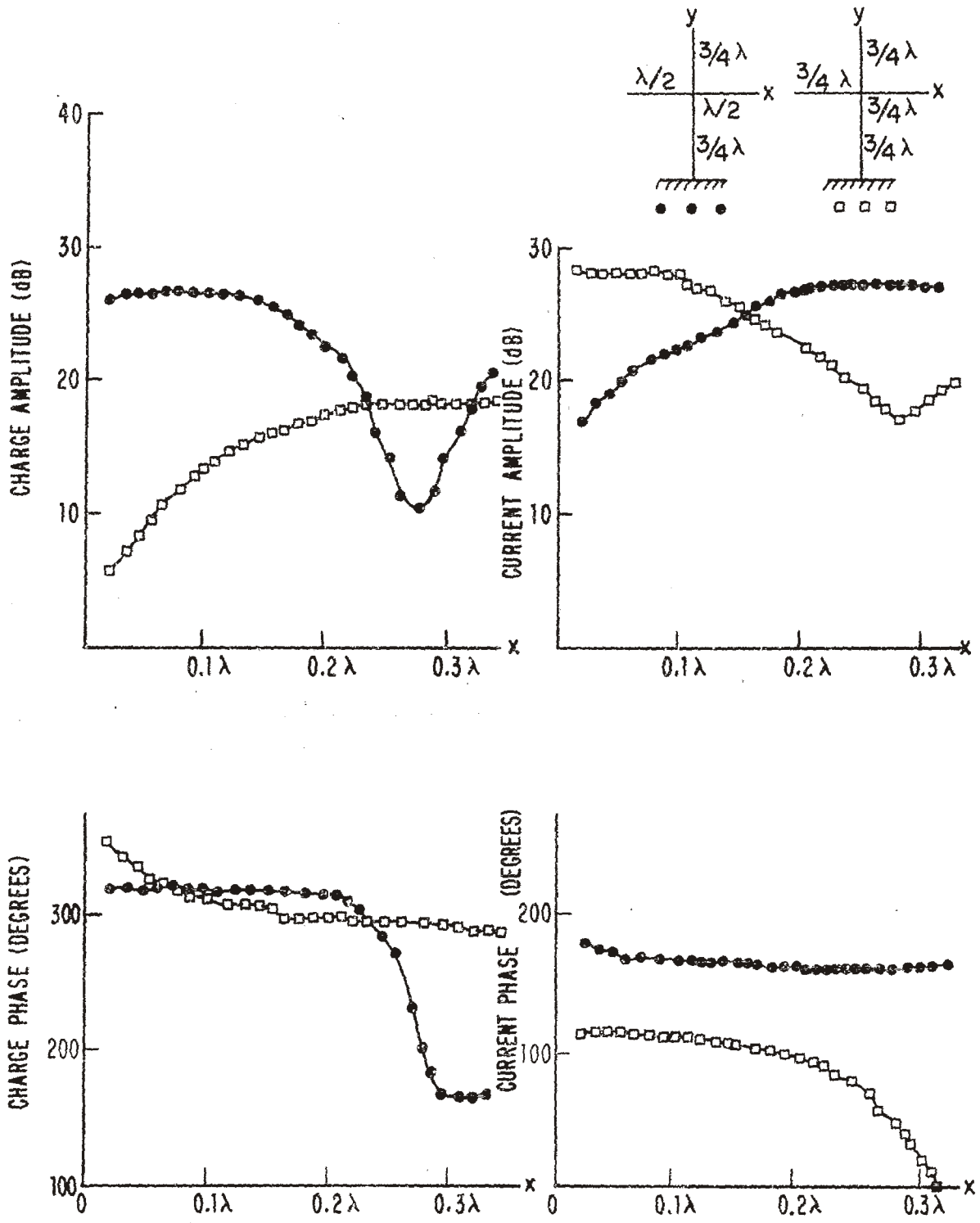

AMPLITUDE AND PHASE DISTRIBUTIONS OF CHARGE AND LONGITUDINAL CURRENT DENSITY ON HORIZONTAL ELEMENT OF CROSS DIPOLE RECEIVING ANTENNA ILLUMINATED BY A VERTICALLY POLARIZED PLANE WAVE AS A FUNCTION OF DISTANCE (WAVELENGTHS) MEASURED FROM JUNCTION. (CASE 6)

FIGURE 21

The degree of interaction between the horizontal cross arms and the vertical member is determined by the magnitude of the current and charge in the junction region of the parasitic monopole and the new resonant conditions brought into being by the addition of the cross arms. Case 1, described in figures 10 and 11, clearly demonstrates this resonance between the vertical and horizontal cross arms with a condition of charge minimum/current maximum existing at the junction, whereas Case 2 (figures 12 and 13) portrays the marked difference occurring when the horizontal cross arm is antiresonant. A similar situation is observed in Case 3 for a condition of charge minimum/current minimum when the horizontal cross arms are varied from a half-length of $\lambda/4$ to $\lambda/2$ (figures 14 and 15). For conditions of charge maximum/current minimum on the parasitic monopole (Cases 4 and 5), significant perturbations in both charge and current densities are observed which demonstrate the interaction of resonant lengths when the horizontal cross arms are added (figures 16 through 19). Case 6 presents an interesting observation of an intermediate case wherein situations of resonance and antiresonance between horizontal and vertical members are highlighted (figures 20 and 21).

It should be noted that the initial data point on the horisontal cross arms, $x \approx 0$, was taken on the front surface of the horizontal arm directly over the edge of the vertical cylinder projected through the junction region. Therefore, it should be observed that using the longitud-

inally oriented current probe, the measured current in this area does not show the transverse components of the currents in the immediate junction region until they blend into longitudinal components several radii out along the horizontal arm.

V. Conclusions

The existence of standing waves of both current and charge on the parasitic monopole gives rise to situations in which sizable currents and/or charges may be observed in the junction region of a crossed-dipole receiving antenna. When horizontal cross arms are added to the vertical parasitic monopole illuminated by a vertically polarized monochromatic plane wave, charges and currents are coupled to these horizontal members. The amount of coupling is a function of both the charge and current present at the location of the junction on the parasitic monopole and the new resonant lengths which occur from the addition of the cross arms. Experimental results have been presented which demonstrate these standing waves and resonant interactions.

Recently, in conjunction with this work, King and Wu have provided a complete analytic solution for the electrically thin crossed dipole which employs corrected boundary conditions and a new integral-differential equation developed in terms of trigonometric functions of the various arm lengths of the crossed dipole (King, R. W. P. and Wu, T. T., to be published). Preliminary comparisons of this theory with the experimental results presented in this paper show close agreement and will be the subject of a sequel to that paper (Burton, R. W. and King, R. W. P., work in progress). The expansion of the distributions in terms of trigonometric functions of arm lengths clearly demonstrates that some combinations of individual arm lengths bring certain sine

and cosine terms into play especially at resonances and antiresonances, thus explaining the experimental interactions observed.

REFERENCES

1. Burton, R. W. and King, R. W. P., to be published, "Currents and Charges on Cylinders in an Electric Field."

2. Burton, R. W. and King, R. W. P., work in progress, "The Crossed Dipole: Theory and Experiment."

3. Butler, C. M., 1972, "Currents Induced on a Pair of Skew Crossed Wires," IEEE Trans. Antennas Propagat., vol. AP-20, pp. 731-736.

4. Chao, H. H. and Strait, B. J., 1972, "Radiation and Scattering by Configurations of Bent Wires with Junctions," IEEE Trans. Antennas Propagat., vol. AP-19, pp. 701-702.

5. Kao, C. C., 1969, "Three-Dimensional Electromagnetic Scattering from a Circular Tube of Finite Length," J. Appl. Phys., vol. 40(12), pp. 4732-4740.

6. King, R. W. P., 1956, Theory of Linear Antenna. Cambridge, Mass.: Harvard University Press, Chapter IV; Chapter III.

7. King, R. W. P. and Wu, T. T., to be published, "Analysis of Crossed Wires in a Plane-Wave Field."

8. Mei, K. K., 1965, "On the Integral Equations of Thin Wire Antennas," IEEE Trans. Antennas Propagat., vol. AP-13, pp. 374-378.

9. Taylor, C. D., 1969, "Electromagnetic Scattering from Arbitrary Configuration of Wires," IEEE Trans. Antennas Propagat., vol. AP-17, pp. 662-663.

10. Taylor, C. D., Lin, S. M., and MC Adams, H. V., 1970, "Electromagnetic Scattering from Crossed Wires," IEEE Trans. Antennas Propagat., vol. AP-18, pp. 133-136.